Journal of Applied Biosciences 214: 22773 – 22787
ISSN 1997-5902

Mapping land use and soil salinity using multispectral data from Landsat sensors in the municipality of Fimela (Fatick, Senegal)

Hyacinthe SAMBOU[1*], Seyni SANE[2], Cheikh Sadibou FAYE[3]
1.Institute of Environmental Sciences, Cheikh Anta Diop University of Dakar, Senegal. hyacinthe.sambou@ucad.edu.sn
2 Higher Institute of Professional Education (ISEP) in Bignona, Senegal. sane.seyni@gmail.com
3 Civil Engineering Department, Thiès Polytechnic School (EPT). csfaye@ept.edu.sn

Submitted 10/09/2025, Published online on 30/11/2025 in the https://www.m.elewa.org/journals/journal-of-applied-biosciences-about-jab/ https://doi.org/10.35759/JABs.214.8

ABSTRACT
Objective: This study aims to analyse the vulnerability of the agricultural sector to salinization caused by climate variability in the municipality of Fimela.
Methodology and results: The methodology is based on the processing of Landsat satellite images from 1973, 1990, 2007, and 2024 to determine the evolution of landscape units in relation to key climatic events. In addition, multispectral bands from the Landsat sensor were used to calculate soil and vegetation salinity indices to characterize soil salinity levels. Similarly, socioeconomic surveys were conducted among farmers. Soil sample analyses were carried out, as well as rainfall data collection. The results showed a 7.57% increase in mudflats between 1973 and 2024 and a 1.84% decrease between 1990 and 2024. In contrast, agricultural land decreased by 7.52% between 1973 and 2024. Salinity Index (SI5), Salinity Index 3 (SI3), and the Vegetation Soil Salinity Index (VSSI) yielded the best results for assessing soil salinity with a coefficient of determination r2 of 0.65. However, indices vary depending on soil type and land cover units. Since multispectral bands, such as green (G), red (R), and near-infrared (NIR), are available on many existing satellite sensors, such as Landsat and Sentinel, the concept of determining soil salinity indices can be extended in the long term for monitoring soil salinization.
Conclusion and application of results: The results of this study enable researchers to develop methods to supplement conventional soil characterization and monitoring methods, which are often costly. They also enable agricultural sector agents to move towards new methods of combating degradation and restoring degraded land in Senegal.
Keywords: Dynamics, agricultural land, satellite imagery, salinity index, Senegal

INTRODUCTION

Senegal, like most countries in sub-Saharan Africa, is an agricultural country. The availability of arable land has enabled the development of the agricultural sector, which has become one of the drivers of national economic growth. At present, despite some difficulties, agriculture (subsistence, industrial, and export) remains a major component of the Senegalese economy. It accounts for 8.4% of gross domestic product (GDP) (National Agency for Statistics and Demography, ANSD, 2011) and contributes to GDP growth of around 0.5% (ANSD, 2011). Furthermore, employing 60% of the working population (ANSD, 2009), agriculture is the main source of livelihood for rural populations. More than 3 out of 5 Senegalese depend on the agricultural sector (FAO, 2011). However, agriculture is highly vulnerable to several factors such as erosion, lack of fertilizers, desertification, and climate change. Among these factors, the impact of climate change appears to be the most significant. Most of the populations in sub-Saharan Africa are particularly exposed to climate risks, as they are heavily dependent on rain-fed agriculture, which accounts for nearly 93% of cultivated land (Sultan. 2015). In Senegal, the agricultural sector is heavily dependent on climatic conditions, particularly rainfall. In addition, the consequences of climate change are affecting several key sectors of the economy. These include, among other things, the anticipated impacts on agriculture due to soil and groundwater salinization, which will accelerate the formation of tannins and reduce arable land. Globally, salinization is a type of land degradation that affects a total area of 800 million hectares, or nearly 4% of the world's land surface (FAO, 2009). The total area of land affected by salt in Senegal is estimated at 800,000 ha, a significant portion of which is in the Fatick region (ISRA, 2011). This region is therefore one of the areas where soil salinization is most widespread in Senegal (Chauvin, 2013). This salinization leads to the gradual degradation of large areas of land. In the Saloum Islands, particularly in the estuarine areas of Fimela, which, due to its geographical location and insular nature, is one of the most vulnerable territories. As a result, soil salinization has become a veritable ecological disaster, with a sharp increase in areas that are barren, oversalted, hyper acidified, and unsuitable for cultivation. (CNRF, 2012). This degradation also has an impact on the lack of arable land and declining productivity. This study aims first to analyse the spatio-temporal dynamics of soil salinization in the municipality of Fimela and to determine salinity indices based on satellite images. The goal is to identify indicators that can be used to determine soil salinity levels in the absence of laboratory analyses of samples taken in the field.

MATERIALS AND METHODS

Descriptions of the Study Areas: The municipality of Fimela is located in central-western Senegal. Geographically, it is located between 13°59' 30“ N and 14°11'30” N and between 16°30' 00“ W and 16°48' 00” W (Figure 1). The study area covers 31,514 hectares. The municipalities of Dioffior, Dionewar Djilasse, Djilor, Djirnda, Loul Sessene, Mbam, Nguediene, and Palmarin Facao surround the municipality of Fimela. Climate plays an important role in the salinization process. In the municipality of Fimela, the climate is Sudanian-Sahelian, with rainfall varying between 400 and 600 mm. The soils are tropical, ferruginous, unwashed dior soils. There are also sandy, deep soils, Deck soils in hydromorphic interdune depressions, leached tropical ferruginous Deck-dior soils and sandy-clay soils, and slightly leached ferralitic soils (Banabessey, 2011). The

vegetation in the municipality is highly diverse in terms of flora, depending on rainfall, soil type, and human activity (Mbaye, 2013).

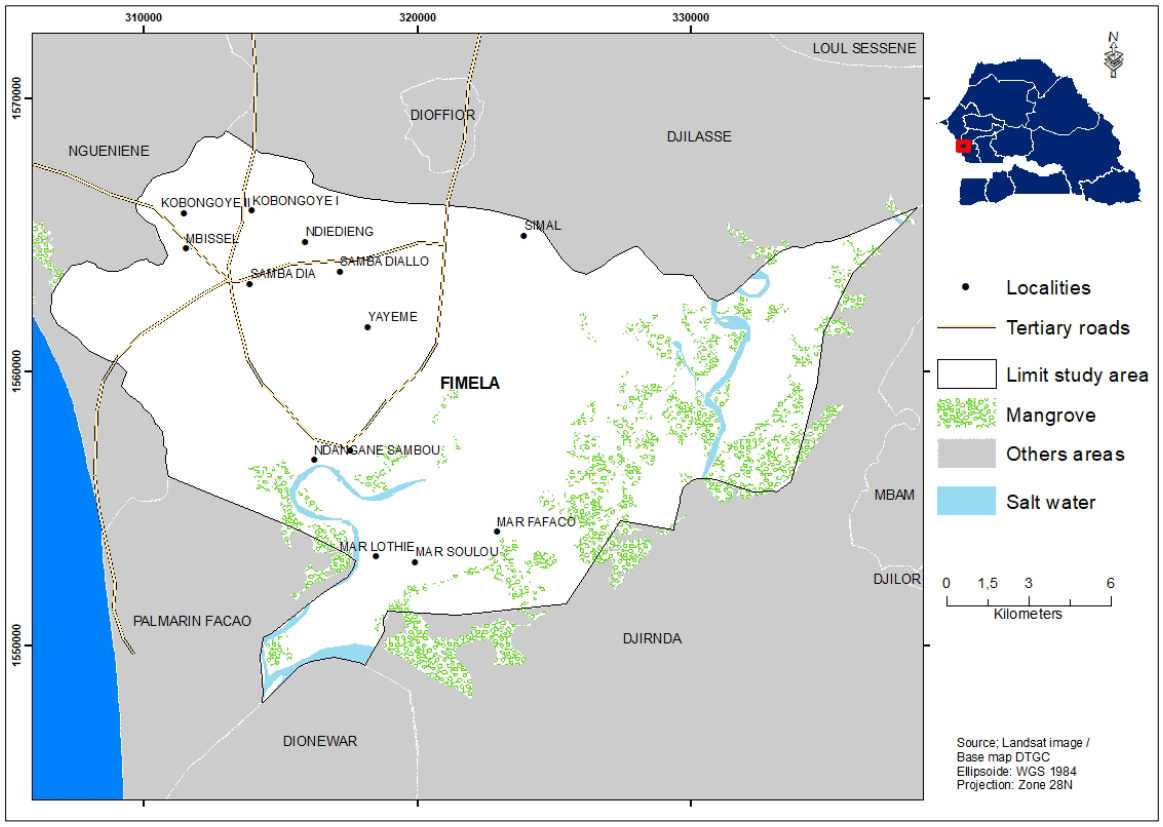

Figure 1: Location map of study area

Image data collection: The Landsat scenes for February covering the study area were downloaded from the United States Geological Survey (USGS) archives at http://earthexplorer.usgs.gov/ for the purposes of this study. The scenes were selected during the post-rainy season, which is favourable for good discrimination of land use units in the Sudano-Sahelian zone (Zoungrana *et al.,* 2018). Thus, all processed satellite images were taken in March.

Preprocessing of acquired satellite images: The satellite images selected for this study will undergo a number of processes that will enable us to map the changes that have taken place in the municipality of Fimela. The images used are from Landsat sensors. These are the Multispectral Scanner (MSS) for the 1973 image, the Thematic Mapper (TM) sensor for the 1990 image, the Enhanced Thematic Mapper (ETM+) for the 2007 image, and the Operational Land Imager (OLI) sensor for the 2024 image. According to Stellmes *et al.* (2010), 30 m resolution can reveal changes at the local level. All images were calibrated using image 2024 as a reference. Twenty (20) landmarks (corresponding points between the reference image and the other images acquired) were used in this exercise. This geometric correction has improved image quality and made the spatial entities present in the images closer to the real world (Caloz and Collet, 2001). The nearest neighbour resampling method and geometric correction were used in conjunction with a first-order polynomial transformation to resample the

1973 image, which has a resolution of 58 m. The validity check was assessed by estimating the standard error, RMSE (Root Mean Square Error) or Mean Square Error. Since RMSE is only an indicator, the validation of geometric corrections will be supplemented by a visual check performed by superimposing the images. The spatial accuracy threshold used was equivalent to an error of less than one pixel. The images are then enhanced by spreading the dynamics and false colour compositions (4-3-2) for the MSS sensor image, (5-4-3) for the ETM+ sensor images, and (6-5-4) for the OLI sensor to be created for better interpretation of the image themes. This choice is explained by the fact that visible and near-infrared wavelengths alone contain 90% of the spectral information relating to living vegetation (Baret *et al.,* 1988).

Image processing: Supervised classification: To conduct this study properly, field missions were carried out regularly throughout 2024 based on land use units described in the field. A maximum likelihood classification (Diallo *et al.,* 2011; Tra Bi, 2013) resulted in a land use map for the municipality of Fimela. As for supervised classification, it was based on a few points from the training sessions visited during field surveys used for training (Sangne *et al.,* 2015). Supervised classification consists of grouping landscape units with the same spectral response into a single class known as a "thematic class." To obtain a thematic class, areas of interest called training patches are collected from across the image. These plots will be selected so that they have the same radiometry and are then automatically grouped into a single class, known as a thematic class, by the software under the operator's control. It requires visual interpretation of the image based on knowledge of the spectral signatures of all the elements that compose it. This process will produce a classified image consisting of several thematic classes from 1973 to 2024, respectively from the sensors and MSS, TM, ETM+, and OLI of the Landsat satellite (Tendeng *et al.,* 2016). The validation of the 2024 image was based on GPS control points collected in the various land use categories during field investigations. The results of the classification of the other images were validated using other results from previous work carried out in the study area (Sow and Seck, 2021; Amar *et al.,* 2024; Ba *et al.,* 2023), which served as controls. Validation was carried out in two phases. The first phase was a thematic validation focused on a visual comparison between the image of the different colour compositions and the classified image (Doumbia *et al.,* 2024). The second phase, called statistical validation, was based on the analysis of the confusion matrix using overall accuracy and the Kappa coefficient. The overall accuracy of the classification is equal to the average of the percentages of correctly classified pixels. According to Congalton (1991), the Kappa coefficient provides a more accurate estimate (which takes into account correctly classified pixels) of the quality of the classification. Thus, the Kappa index evaluates the agreement between the results obtained (map) and the reality on the ground in the confusion matrix (Bogaert *et al.,* 2011).

Sampling for determining salinity and salinity index: The site survey and sample collection were carried out over a period of one month in March 2024. The choice of this period coincides with very low or even non-existent vegetation cover in certain areas of the plain. This period is considered to be a period during which salt accumulation appears to be greater on the soil surface and therefore most easily detectable. The salinity of 107 sampled points and their electrical conductivity (EC) were determined in the laboratory using the 1/5 diluted extract method (USSL, 1954). The samples were taken from a depth of 25 cm. Table 1 was used to interpret the results obtained from laboratory analysis of the soil samples.

Table 1: Classification of soil salinity based on electrical conductivity values (FAO, 2008)

EC dSm^{-1}	Soil salinity classes
< 0.75	non saline
0.75 <EC< 2	slightly saline
2 <EC< 4	moderately saline
4 <EC< 8	strongly saline
8 <EC< 15	very strongly saline
> 15	extremely saline

The sampling method used was stratified sampling. It was based on the classes derived from the processing of the March 2024 satellite image. Each sampled point was georeferenced using a Garmin GPS device. The land use unit for agricultural land has more samples because the focus of our study is more on changes in agricultural land. Figure 2 shows the spatial distribution of the sampling plan carried out in the study area.

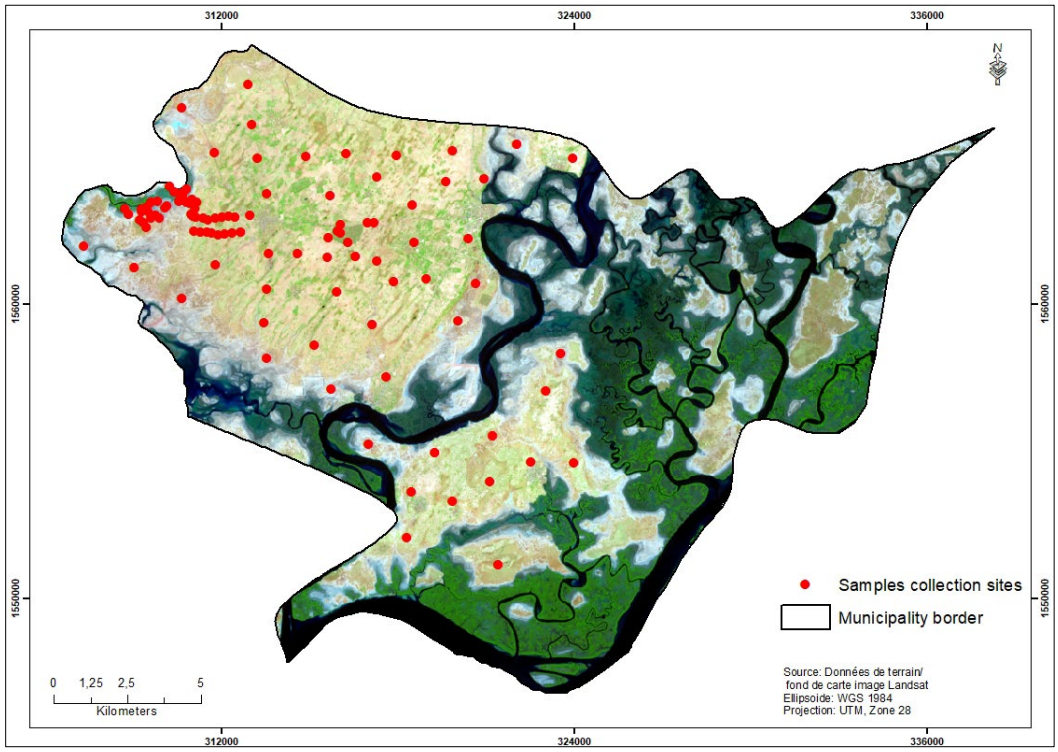

Figure 2: Spatial distribution of soil samples and their measured electrical conductivity

Salinity indices were calculated from the Landsat image of March 13, 2024. The list of indices evaluated can be found in Table 2 below.

Table2: List of evaluated spectral indices

Index	Formulation	References
Vegetation Soil Salinity Index (VSSI)	2G - 5(R + NIR)	Nguyen *et al.,* 2020
Salinity Index (SI)	$\sqrt{(B \text{ x } R)}$	Khan *et al.,*2005
Normalized Differential Salinity Index (NDSI)	$(R - NIR)/(R + NIR)$	Khan *et al.,* 2005
Salinity Index 1 (SI1)	$\sqrt{(G \text{ x } R)}$	Douaoui *et al.,* 2006
Salinity Index 2 (SI2)	$\sqrt{(G^2 \text{ x } R^2 + NIR^2)}$	Douaoui *et al.,* 2006
Salinity Index 3 (SI3)	$\sqrt{(G^2 + R^2)}$	Douaoui *et al.,* 2006
Salinity Index (SI5)	(B × R) / G	Abbas and Khan, 2007
Intensity Indices-Int1	(G + R)/2	Fourati *et al.,* 2015
Intensity Indices-Int2	(G + R+NIR)/2	Fourati *et al.,* 2015
Normalized Difference Vegetation Index (NDVI)	(NIR - red)/(red + NIR)	Khan *et al.,* 2001
Soil Adjusted Vegetation Index (SAVI)	(1 + L) × NIR - red/L + NIR + red (L = 0.5)	Alhammadi and Glenn, 2008

B: Blue band, G: green band, R: red band, NIR: Near infrared band for Landsat image

Rainfall data: Annual rainfall data from the Fatick station from 1981 to 2024 were processed. The purpose of this study is to understand the potential impacts of rainfall variability in the study area on land use dynamics, particularly the dynamics of saline soils. The Pettit Test was selected for use in this study.

RESULTS

Land use dynamics between 1973 and 2024: The statistical evolution of the different land use units in the municipality of Fimela between 1973 and 2024 is presented in Table 3. This table is derived from the analysis of Figures 3 and 4.

Table 3: Statistics on land use dynamics

Classes	1973		1990		2007		2024	
	Area (ha)	Area (%)	Area (ha)	Area (%)	Area (ha)	Area (%)	Area (ha)	Area (%)
Water	1878.45	5.38	3261.31	9.35	3201.32	9.18	4829.58	11.5
Mangrove	2756.66	7.9	1705.56	4.89	1897.73	5.44	3421.87	8.14
Tans	6972.63	20	4562.21	13.08	4252.23	12.2	2705.5	6.44
Mudflats	9349.79	26.82	11988.87	34.39	11346.08	32.55	8945.87	21.3
Land vegetation	3526.73	10.11	6073.43	17.42	3837.41	11.01	10245.99	24.4
Habitation			180.85	0.51	390.52	1.12	2486.01	5.92
Agricultural land	10368.84	29.75	7080.85	20.31	9927.76	28.48	9353.71	22.27

Land use between 1973 and 1990: The results of land use dynamics between 1973 and 1990 (Figures 3A and 3B) showed that agricultural land and mudflats were the most significant land use categories, covering 10,368.84 ha and 9,349.79 ha respectively, or 29.75% and 26.82% of the total area of the study zone (Table 3). With 6,972.63 ha, or 20%, tans also occupied a significant area within the study zone. Due to the spatial resolution of the 1973 image (58 m) and the type of construction materials, the housing class could not be clearly visualized in the 1973 image.

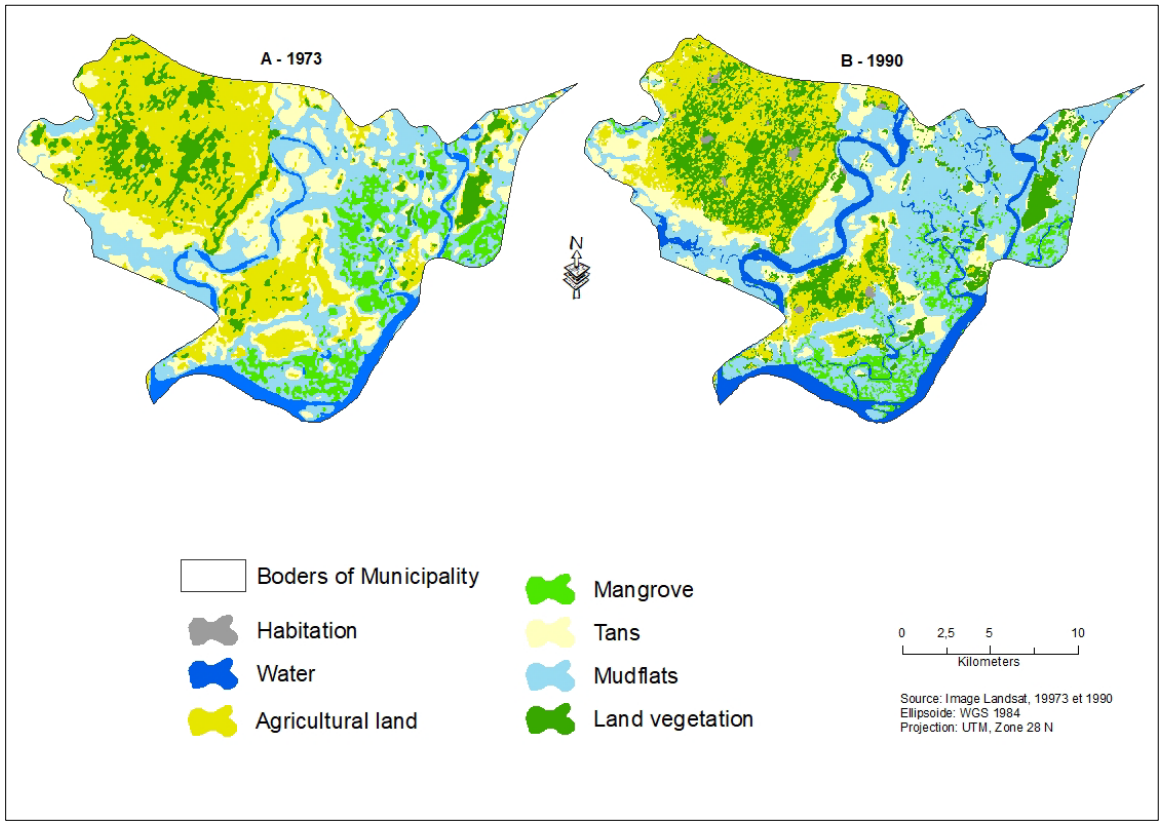

Figure 3: Land use map of the municipality of Fimela from 1973 and 1990

Land use between 1990 and 2007: Between 1990 and 2007, all land use categories experienced a decline in area except for vegetation, mudflats, and water. Thus, the areas of agricultural land and pastures decreased by 9.44 ha and 6.92 ha, respectively (Table 3). However, the areas covered by vegetation and mudflats have increased significantly, by an estimated 7.42 ha and 7.57 ha respectively. However, the quality of the 2007 image, with its resolution of 30 m, made it possible to estimate the area occupied by dwellings. In 2007, this was estimated at 180.85 ha.

Land use between 2007 and 2024: The diachronic study of land cover between 2007 and 2024 shows a notable change in the surface area of certain land use units, as shown in Figures 4C and 4D. Analysis of Table 3 shows that the areas covered by dwellings, land vegetation and mangroves increased between 2007 and 2024. Thus, land vegetation increased by 13.39%, mangroves by 2.7%, and dwellings by 4.8%. In addition, certain land use units, particularly agricultural land, mudflats and tans have declined. This decline is estimated at 6.21% for agricultural land. Mudflats and tans, meanwhile, have seen an estimated loss in area of 11.25% and 5.76% respectively. Overall, in the municipality of Fimela, land use units increased slightly between 1973 and 2024, with the exception of agricultural land, which declined in area during this period.

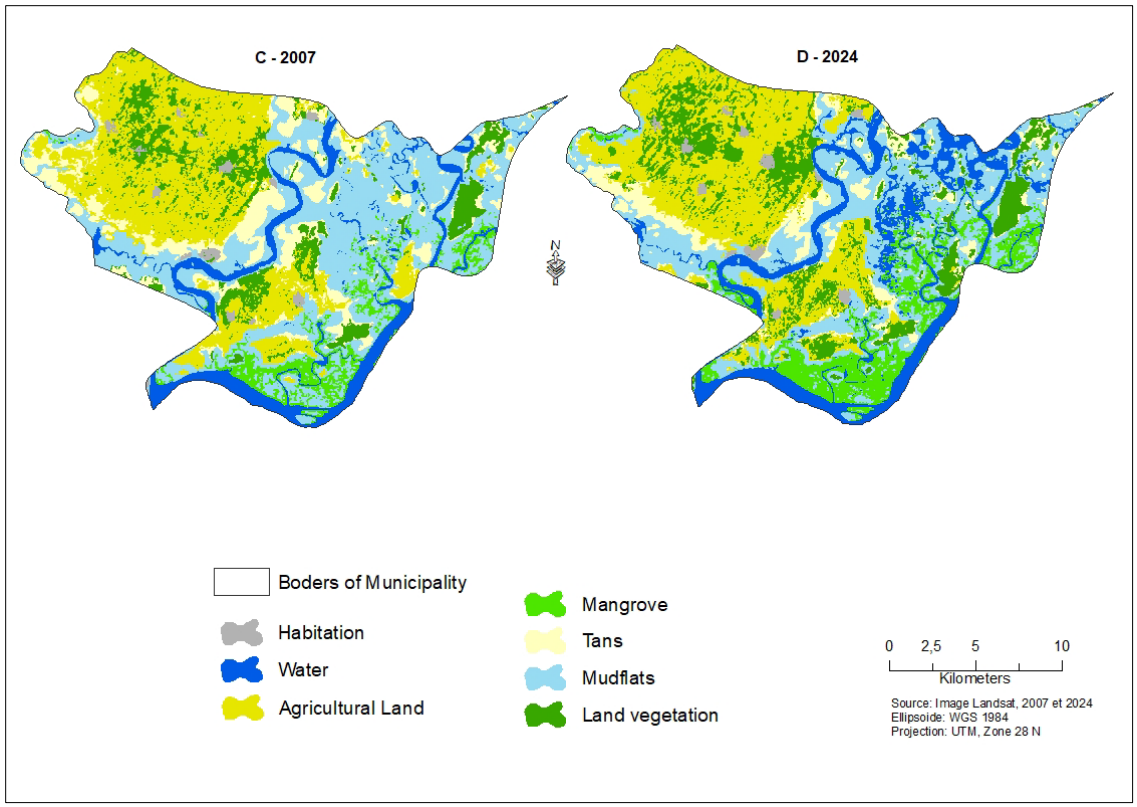

Figure 4: Land use map of the municipality of Fimela for 2007 and 2024

Analysis of electrical conductivity in the ground : Five salinity classes were selected based on electrical conductivity values, using the soil salinity classification system of the Food and Agriculture Organization of the United Nations (FAO, 2008), as shown in Table 1. Table 4 contains summary statistics of soil electrical conductivity measurements for all composite samples collected from the three sites. Electrical conductivity values ranged from moderately saline to non-saline. Overall, the non-saline class (EC < 2 dS/m) was dominant in the study area. It accounted for approximately 52.63% of the total samples. The moderately saline class, 2–4 dS/m, and the highly saline class, 4–8 dS/m, with 17.54% and 15.80% respectively, follow it. However, the degree of salinity differs depending on the land use units. Thus, 77.78% of the agricultural land sampled is non-saline, 11.22% is slightly saline, and 11.22% is moderately saline, while for terrestrial vegetation, 78.94% of the samples are non-saline, 15.79% are slightly saline, and 5.27% are moderately saline. Furthermore, the highest electrical conductivity is recorded in mudflats, tans, and mangroves. In these land use units, more than 75% of the land is moderately to highly saline.

Table 4: Maximum (MAX), minimum (MIN), Mean, and standard deviation (SD) values for actual electrical conductivity (EC) and salinity indices

Land use units		EC (dS/m)	NDSI	SI5	SI	SI2	SI-3	VSSI	Int1	Int2	BI
Agricultural land	Mean	0.580	0.17	20839	1276052	25241	17341	-133769	12237	21407	24751
	SD	1.021	0.02	1255	57456	1055	734	6247	512	860	977
	Max	3.440	0.21	22594	1378185	26876	18556	-118871	13084	22805	26145
	Min	0.17	0.14	17963	1158914	22723	15720	-143329	11104	19308	22571
Mangrove	Mean	4.446	0.23	13425	918395	18923	12758	-95834	9018	16060	17959
	SD	1.941	0.04	523	31925	449	403	2879	286	333	801
	Max	7.67	0.28	14241	989391	19640	13416	-90467	9486	16386	19148
	Min	2.11	0.18	12444	889338	18142	12317	-100368	8706	15447	17000
Tans	Mean	2.63	0.12	20849	1478988	26720	19303	-138997	13623	22857	25600
	SD	1.675	0.02	1819	64337	1291	763	8592.9	534	1059	1024
	Max	4.62	0.14	22265	1551151	28185	20284	-123159	14309	24093	27210
	Min	0.26	0.09	17402	1394671	24483	18379	-147646	12987	21075	24023
Land vegetation	Mean	0.344	0.20	17445	1091936	22267	14908	-116505	10533	18786	22492
	SD	0.631	0.03	1136	88670	1030	1061	6194.06	744	929	1173
	Max	2.07	0.27	19007	1199515	24062	16245	-105958	11472	20292	25198
	Min	0.007	0.16	15326	931246	20608	13094	-128069	9256	17330	20916
Mudflats	Mean	3.317	0.11	16756	1299837	23342	17100	-118207	12148	20038	22201
	SD	2.003	0.02	2701	180284	2796	1841	16402	1369	2369	2951
	Max	5.78	0.14	20220	1486526	26700	18712	-95539	13478	22810	24997
	Min	0.774	0.10	12995	1030217	19379	14211	-139191	10048	16636	17506

Analysis of spectral indices for estimating soil salinity

Multiple linear regression: Soil salinity indices vary according to soil type and land use and occupation units. Thus, multiple linear regression was used to study the implications of the independent variables (11 different indices) on the dependent variable of electrical conductivity (EC). Variable selection (stepwise method) identified four (04) spectral indices that have an impact on electrical conductivity (Table 4).

Table 4: Regression coefficients

Coefficients	Estimate	Std. Error	t value	Pr(>|t|)	Significativité
(Intercept)	-8.287e+03	5.077e+03	-1.632	0.108794	
SI5	-9.416e-01	2.654e-01	-3.548	0.000843	***
SI_3	2.850e+00	8.905e-01	3.201	0.002361	**
VSSI	-2.934e-02	1.086e-02	-2.701	0.009350	**
NDSI	3.834e+04	1.468e+04	2.613	0.011779	*
SI2	-1.099e+00	7.144e-01	-1.538	0.130264	
SAVI	-4397	25616	-0.172	0.8644	
NDVI	2343	39469	0.059	0.9529	

F(5,51) = 18.7, p-value = 1.636e-10, r^2 = 0.65

In fact, with the exception of the SI2 index, all other spectral indices have a significant effect on CE. Thus, the SI5, VSSI, and SI2 indices have a negative influence on CE (Figure 5). A one-unit increase in these indices results in a decrease in CE of 0.9, 0.03, and 1.1 times, respectively. On the other hand, the SI_3 and NDSI indices have a positive effect on CE (Figure 5). Their increase causes an increase in the EC of 3 and 38,300 times, respectively. Furthermore, the F-test (F) indicates that the model is globally significant, and the coefficient of determination r2 of 0.65 means that 65% of the variability in EC is explained by the spectral indices included in the model, while 35% is due to other factors not included in the model.

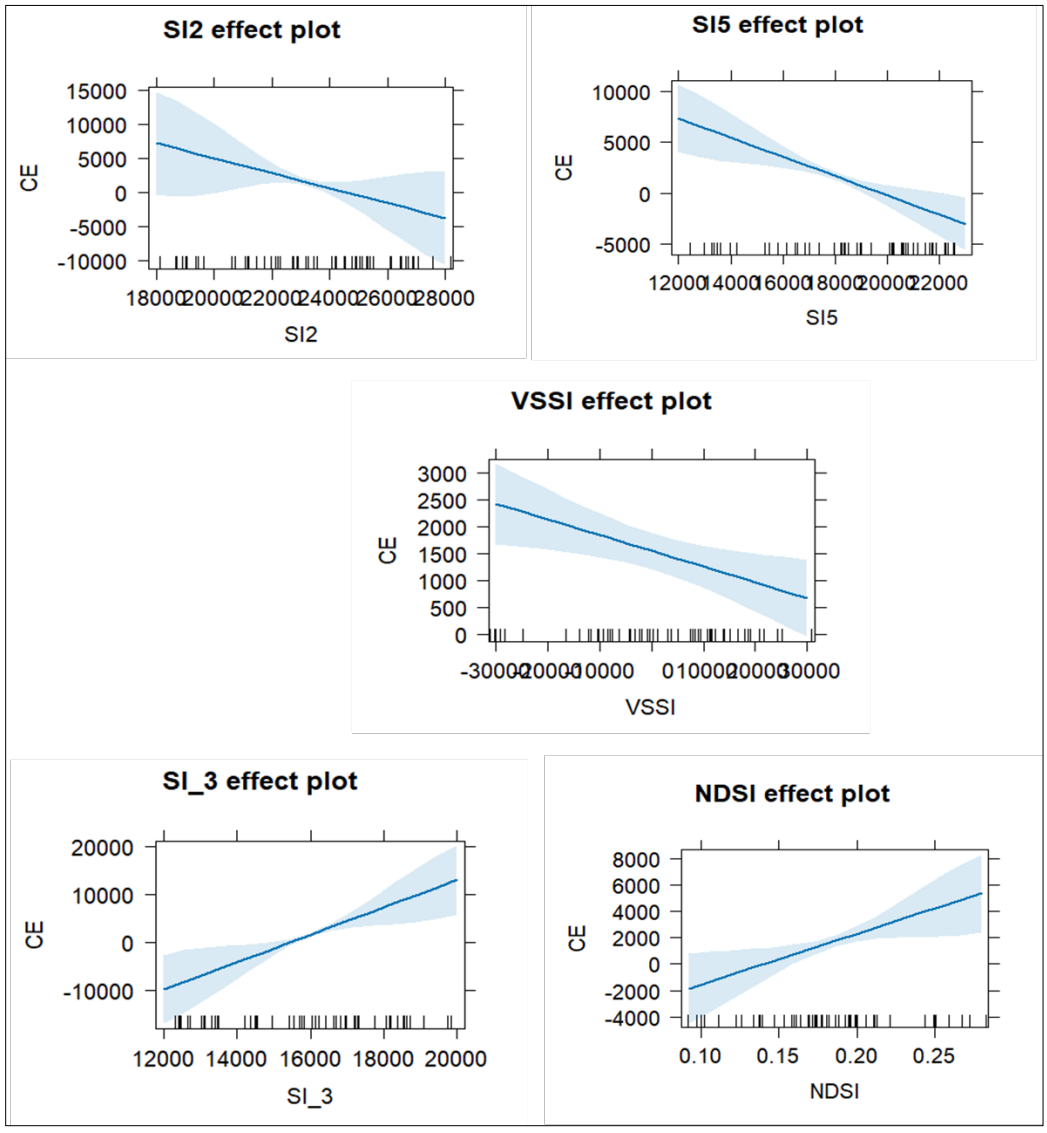

Figure 5: Linear adjustment graphs of the EC with the SI5, VSSI, SI2, SI_3, and NDSI indices

Analysis of rainfall data: The Pettit Test revealed a significant change in the rainfall series at the Fatick synoptic station, which covers our study site. Figure 6 shows a break that marks the sharpest discontinuity in the time series. This was observed in 2007.

However, the period from 2008 to 2021 marks a gradual return to normal rainfall levels. Nevertheless, this recovery remains below the normal levels recorded during the period from 1961 to 1971.

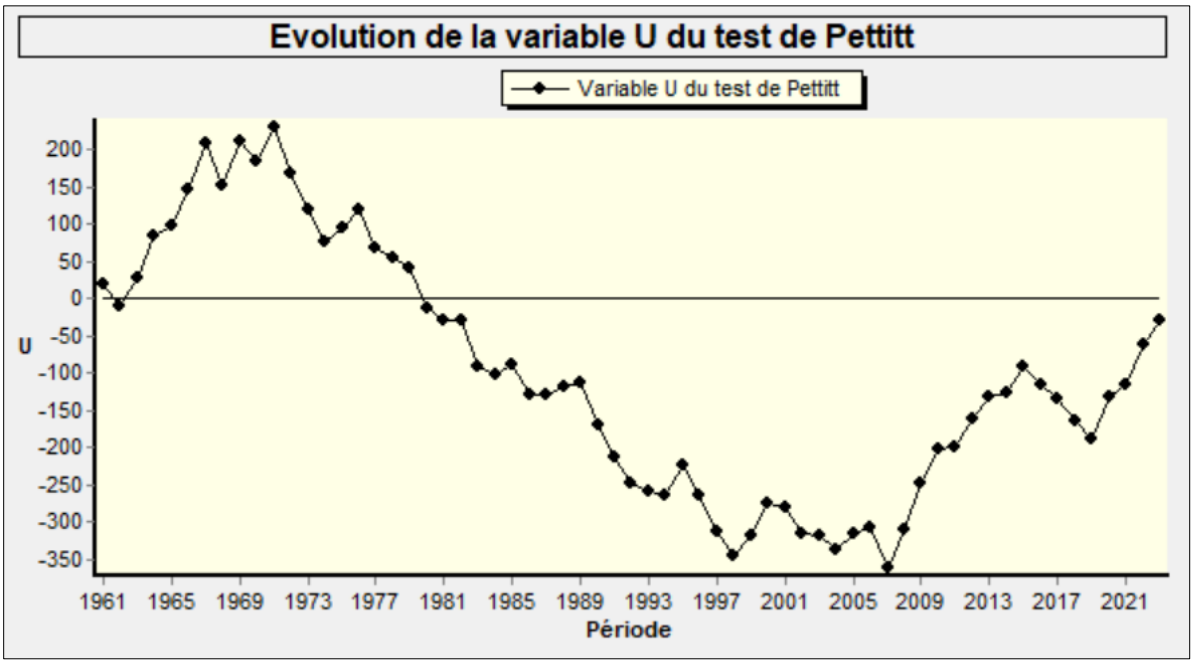

Figure 6: Pettit test showing break dates in rainfall series for the period 1940-2013, Fatick rainfall station

DISSCUSSION

The processing of Landsat satellite images using the maximum likelihood algorithm in ENVI 5.6 software, combined with field observations and the results of previous work carried out in the study area, has enabled seven land cover units to be identified. The units selected consist of the frame, agricultural lands areas, mudflats, tans, mangroves, land vegetation and water. However, the spatial resolution of the 1973 image (58 m) did not allow for clear distinction of the built-up land use unit, which explains its absence in 1973. In this study, land cover units were classified with significant statistical accuracy (Kappa index between 0.85 and 0.95%), resulting in a very satisfactory land cover classification rate (Pontius, 2000, N'Guessan 2018). In addition, slight confusion was noted between tans and agricultural areas. However, the percentage of confusion between these two classes remains low at around 5%. This confusion is certainly linked to the difficulty of visually distinguishing between these two classes during the dry season due to their similar spectral signatures. As the images were taken during the dry season, most agricultural areas are heavily farmed and, in addition, in the study area, after harvesting, residues are collected to be sold as livestock feed. This situation leaves the soil completely bare, resembling tans (Sambou, 2015). Changes in land cover units often depend on atrophic and climatic factors (Faye *et al.,* 2019; Sow *et al.,* 2021). Analysis of satellite images has thus revealed a general trend in the dynamics of land cover units. This trend shows an increase in the area of mudflats, which rose from 9,349.79 ha, 11,988.87 ha, and 11,346.08 ha in 1973, 1990 and 2007, respectively. This increase has been at the expense of mangroves and agricultural areas, which have seen their surface areas decline by 3.01% and 9.44%

between 1973 and 2007. These results corroborate those of Ba *et al.* (2023). In addition, a slight increase in mangrove area was detected between 2007 and 2024. Two factors are believed to be responsible for this increase. On the one hand, reforestation activities carried out by farmers' organizations in the area with the support of decentralized government services (Marine Protected Areas service) and non-governmental organizations such as OCEANIUM, and on the other hand, the return of rainfall in the area has allowed for natural regeneration, albeit weak at present. Furthermore, the area of tans decreased by 6.92% between 1973 and 1990. These results are consistent with those of Faye *et al.* (2019). However, contrary to the work of Amar *et al.* (2024), salinity is not necessarily the major factor in the decline in agricultural land area, as the electrical conductivity values found in samples taken from agricultural areas are low. As proof, 78% of them are classified as non-saline. Only 22% are moderately to slightly saline. The slight to moderate salinity observed in agricultural areas could be explained by the fact that farming practices act as a leaching system for these soils (Allbed *et al.,* 2014). However, to combat this salinity, numerous actions have been undertaken by state structures to combat the salinization of agricultural land. Projects promoting land recovery have been launched, such as the ISRA/Enabel agreement in the municipalities of Djilor Djidiack, Loul Sessene, Baboulaye, etc. (ISRA report, 2019). The results of Pettit's rainfall breakpoint test at the Fatick station show a recovery in rainfall from 2008 onwards after a long period of deficit between 1971 and 2007. These results confirm those of Sow *et al.* (2019), which indicate the impact of rainfall variability on the dynamics of mangroves and land in the Saloum Delta Biosphere Reserve, the area where our study site is located. The results obtained from calculating salinity indices reveal that the indices vary according to land use units. Multiple linear regression analysis showed that the relationships between soil salinity and the indices used in this study yielded conclusive results. Thus, in our study area for the nine indices determined, only the S5, SI-3, VSSI, and NDSI indices have an influence on soil salinity. However, these indices do not have the same influence on the estimation of saline soils. Thus, the NDSI and SI3 indices have a positive influence on soil salinity. The higher the value of these indices, the higher the salinity level. On the other hand, the VSSI, SI2, and SI5 indices have a negative influence on soil salinity. The results recorded from these indices are thought to be due to the wavelengths of the red (R) and near-infrared (NIR) bands used to characterize soil salinity, such as surface crust (Metternicht and Zinck, 2008). Zhang *et al.* (2011) state that the red and NIR spectral regions have proven to be relevant for identifying soil minerals that form during salt stress and in crusts. On the other hand, the BI, Int2, and SI2 indices have virtually no influence and therefore cannot be used to determine the degree of soil salinization, as shown by the linear regression model. This result is like that found by (Zhang *et al.,* 2022). The NDSI index found in our study area has an influence on soil salinity, although this influence is weak. This result confirms that of Khan *et al.* (2005), who concluded that the NDSI index is a relevant index for determining different salt concentrations on the soil surface. Furthermore, Bannari *et al.* (2008) believed that the NDSI index was a poor indicator of salt concentrations since, in their study, NDSI had no influence on the characterization of salinity. However, the NDVI and SAVI vegetation indices yielded inconclusive results for estimating soil salinity in our study area. These results are likely related to the status of land use of our study area, more specifically to the varying density of vegetation cover. The density of vegetation cover was insufficient to assess soil salinity. However, Bouaziz *et al.* (2011) and Fan *et al.* (2012) found that the

SAVI, NDVI, and EVI vegetation indices were weakly correlated with EC values due to insufficient vegetation cover density. The results relating to the use of salinity and vegetation indices for characterizing soil salinity showed that certain indices produced relatively conclusive results. However, we believe that the correlation between the indices and soil salinity depends on climatic, pedological, and environmental conditions, as these vary depending on the study area and land use types. As a result, no single index can provide satisfactory results in all climatic and environmental conditions.

CONCLUSION AND APPLICATION OF RESULTS

The main conclusions drawn from this study are summarized below. Land occupation and use dynamics in the municipality of Fimela are strongly linked to natural factors such as rainfall deficit and soil salinization due to salt intrusion, as well as anthropogenic factors such as overexploitation of land, particularly agricultural land, and destruction of vegetation cover. These factors contribute to the salinization of agricultural land, leading to a reduction in arable land. However, strategies developed to recover salt-affected soils in the municipality are beginning to yield positive results. This is reflected in a reduction in the area occupied by salt marshes between 2007 and 2024. This study showed compatibility between satellite data and field data in estimating soil salinity. However, using these indices in other study areas may yield different results, as their performance varies depending on soil type and land use. The results of this study showed that it would be desirable to prioritize the SI5, SI2, VSSI, and NDSI indices in estuarine areas and fluvial-marine ecosystems to estimate soil salinity levels. The vegetation indices NDVI and SAVI did not yield satisfactory results in this study. In the next phase of this study, we plan to test other satellite sensor data with higher spatial resolution (Sentinel, Pléiade, and drone imagery) in the same area to evaluate the effectiveness of different spectral/spatial resolutions in estimating soil salinity, as they may offer greater accuracy. Similarly, the development of predictive models of soil salinity based on remote sensing indicators and regression techniques should be considered in the future. This would provide researchers with a model that could replace soil analyses, which can sometimes be costly, with the use of satellite images. This study could also help to assess the impact of measures to restore saline agricultural land in the municipality of Fimela.

ACKNOWLEDGEMENTS

We would like to express our gratitude to the residents of Fimela, as well as to the research team who participated in collecting data in the field.

REFERENCES

Abbas A, Khan S, 2007. Using remote sensing techniques for appraisal of irrigated soil salinity. Paper presented at the Advances and Applications for Management and Decision Making Land, Water and Environmental Management: Integrated Systems for Sustainability MODSIM07

Alhammadi MS, Glenn EP, 2008. Detecting date palm trees health and vegetation greenness change on the eastern coast of the United Arab Emirates using SAVI, Int. J. Remote Sens., 2008; vol. 29, no. 6: 1745–1765, https://doi.org/10.1080/01431160701395195

Allbed A, Kumar L, Aldakheel YY, 2024. Assessing soil salinity using soil salinity and vegetation indices derived from IKONOS high-spatial resolution imageries: Applications in a date palm dominated region. Geoderma 230–231 (2014) 1–8. http://dx.doi.org/10.1016/j.geoderma.2014.03.025

Amar B, Mbaye MS, Tine AK, Mall I, Sarr M, Aïdara, Noba K, 2024. Étude de la dynamique de l'occupation des sols du département de Fatick de 1984 à 2020 (Fatick, Sénégal). Journal of Animal & Plant Sciences (J.Anim.Plant Sci. ISSN 2071-7024) Vol.59(2) : 10887 -10898. https://doi.org/10.35759/JAnmPlSci.v59-2.5

Agence Nationale de la Statistique et de la Démographie (ANSD), 2011. Situation économique et sociale du Sénégal en 2010. 358 p.

Agence Nationale de la Statistique et de la Démographie (ANSD), 2009. Situation économique et sociale : Région de Fatick, édition 2008. 127 p.

Ba K, Sambou H, Ndiaye B, Goudiaby A, 2023. Dynamics of Land Salinization in the Commune of Fimela (Fatick, Senegal) from 1973 to 2020. Journal of Geographic Information System, 15, 19-34. https://doi.org/10.4236/jgis.2023.151002

Banabessey K., 2011. Diagnostic environnemental de la filière arachide dans la zone du Bassin Arachidier. Dakar (Sénégal) : CNCR, 2011. http://www .cncr.org/IMG/pdf/Diagnostic_partie_1. pd

Bannari A, Guedon AM, El-Harti A, Cherkaoui FZ, El-Ghmari A, 2008. Characterization of slightly and moderately saline and sodic soils in irrigated agricultural land using simulated data of advanced land imaging (EO-1) sensor. Commun. Soil Sci. Plant Anal. 39 (19–20), 2795–2811. https://doi.org/10.1080/00103620802432717

Bogaert J, Barima YSS, Ji J, Jiang H, Bamba I, Iyongo WML, Mama A, Nyssen E, Dahdouh-Guebas F, Koedam N, 2011. A methodological framework to quantify anthropogenic effects on landscape pattern. Landscape ecology in Asian cultures n°45, Springer, Verlag, New York, 141-167.

Baret F, Guyot G, Bague A, Maurel P, 1988. Complementary of middle-infiared with visible and near-inhed reflectance for monitoring wheat canopies. Remote Sensing of Environment, 26: 213-225.

Bouaziz M, Matschullat J, Gloaguen R, 2011. Improved remote sensing detection of soil salinity from a semi-arid climate in Northeast Brazil. Compt. Rendus Geosci. 343 (11–12), 795–803. DOI : 10.1016/j.crte.2011.09.003

Caloz R, Collet C, 2001. Précis de télédétection-Volume 3: Traitements numériques d'images de télédétection. Presses de l'Université de Québec, 340 p. https://doi.org/10.2307/j.ctv5j018b

Centre National de Recherches Forestières (CNRF0 (2012) Projet Partenariat Multi-acteurs pour l'Adaptation des Populations Vulnérables à la Salinisation des sols induite par les Changements Climatiques au Sénégal. Rapport, 50 p

Chauvin L, 2013. La salinisation des terres dans la région de Fatick (Sénégal): Etendue et conséquences sur les services écosystémiques du système de production agropastoral. Mémoire de master 2 en Sciences de l'Environnement, Institut des Sciences

de l'Environnement, Université Cheikh Anta Diop de Dakar, Dakar, 89 p.

Congalton RG, 1991. A review of assessing the accuracy of classifications of remotely sensed data. Remote Sensing of Environment. 37: 35-46. https://doi.org/10.1016/0034-4257(91)90048-B

Diallo H., Bamba I, Barima YSS, Visser M, Ballo A, Mama A, Vranken I, Kouassi A M, Kouamé KF, Ahoussi KE, Oularé S, Biémi J, 2011. Impacts conjugués des changements climatiques et des pressions anthropiques sur les modifications de la couverture végétale dans le bassin versant du N'ZiBandama (Côte d'Ivoire). Revue. Internationale des. Sciences et Technoogies, 20: 124-146.

Doumbia M., Asseh EE, Delewron RG, Kouassi RH, Traore-Ouattara K, 2024. Cartographie de l'occupation du sol et dynamique de la forêt classée de l'Orumbo-Boka. Journal of Animal & Plant Sciences (J.Anim.Plant Sci. ISSN 2071-7024). Vol.61(1) : 11168 -11177 https://doi.org/10.35759/JAnmPlSci.v61-1.4

Douaoui AEK, Nicolas H, Walter C, 2006. "Detecting salinity hazards within a semiarid context by means of combining soil and remote-sensing data," Geoderma, vol. 134, no. 1/2, pp. 217–230, 2006. DOI: 10.1016/j.geoderma.2005.10.009

FAO, 2011. L'état des ressources mondiales en terre et en eau pour l'alimentation et l'agriculture : Gérer les systèmes en danger. Rapport de synthèse, 49 p

FAO, 2008. Rapport national sur l'état des ressources phytogénétiques pour l'alimentation et l'agriculture : Sénégal. 46 p.

FAO, IIASA, ISRIC, ISS-CSA, JRC, 2008. Harmonized World Soil Database (version 1.0), FAO, Rome, Italy and IIASA, Laxenburg, Austria.

Fan X, Pedroli B, Liu G, Liu Q, Liu H, Shu L, 2012. Soil salinity development in the yellow river delta in relation to groundwater dynamics. Land Degrad. Dev. 23 (2), 175–189. DOI: 10.1002/ldr.1071

Faye B, Tine D, Ndiaye D, Diop C, Faye G, Ndiaye A, 2019. Évolution des terres salées dans le nord de l'estuaire du Saloum (Sénégal). Géomorphologie: relief, processus, environnement, vol.25- n°2 2019. https://doi.org/10.4000/geomorphologie.13125

Khan NM, Rastoskuev VV, Sato Y, Shiozawa S, 2005. Assessment of hydrosaline land degradation by using a simple approach of remote sensing indicators. Agric. Water Manag. 77 (1), 96–109.

Khan NM, Rastoskuev VV, Shalina EV, Sato Y, 2001. Mapping salt-affected soils using remote sensing indicators - a simple approach with the use of GIS IDRISI. Ratio. 5–9

Mbaye MS. 2013. Association mil [Pennisetum glaucum (L.) R. Br.] et niébé (Vigna unguiculata (L.) Walp.: Arrangement spatiotemporel des cultures, structure, dynamique et concurrence de la flore adventice et proposition d'un itinéraire technique. Thèse d'Etat Unique UCAD/BV. 236 p.

Metternicht G, Zinck JA, 2008. Remote Sensing of Soil Salinization: Impact on Land Management. CRC Press, Taylor and Francis, New York. https://doi.org/10.1201/9781420065039

Nguyen KA, Liou YA, Tran H, Hoang PP, Nguyen TH, 2020. "Soil salinity assessment by using near-infrared channel and vegetation soil salinity index derived from Landsat 8 OLI data: A case study in the Tra Vinh Province, Mekong Delta, Vietnam," Prog. Earth

Planet. Sci., vol. 7, no. 1, pp. 1–16, Jan. 2020.

N'Guessan AE, 2018. Dynamique de la végétation et facteurs de reconstitution de la biomasse dans les forêts secondaires : cas de la forêt classée d'Agbo 1 (Sud-Est de la côte d'ivoire). Thèse Doctorat, UFR Biosciences, Université Félix Houphouët-Boigny,, Côte d'Ivoire, 258p.

Pontius JRG, 2000. Quantification error versus location error in compararison of categorical maps. Photogrammetric Engineering and remote Sensing, 8 (66): 1011-1016.

Sangne CY, Barima YSS, Bamba I, N'Doumé CTA, 2015. Dynamique forestière post-conflits armés de la Forêt classée du Haut-Sassandra (Côte d'Ivoire). VertigO, 15(3) : 1-18.

Sambou H, Sambou B, Mbengue R, Sadio M, Sambou PC, 2015. Dynamics of Land use Around the Micro-Dam Anti-Salt in the Sub-Watershed of Agnack Lower Casamance (Senegal). American Journal of Remote Sensing. Vol. 3, No. 2, 2015, pp. 29-36. doi: 10.11648/j.ajrs.20150302.12

SOW EH, Seck D, 2021. Cartographie des unités écologiques des communes de Fimela et de Palmarin (région de Fatick, Sénégal). Journal of Animal & Plant Sciences (J.Anim.Plant Sci.ISSN2071-7024),Vol.50 (3): 9124-9136 https://doi.org/10.35759/JAnmPlSci.v50-3.3

Sow EH, Ba T, Sy BA, 2019. Impact de la variabilité pluviométrique sur la dynamique de la mangrove de la réserve de biosphère du delta du Saloum (Sénégal). Journal of Animal & Plant Sciences (J.Anim.Plant Sci.), 2019. Vol.40, Issue 2: 6619-6635 Publication date 31/05/2019, http://www.m.elewa.org/JAPS; ISSN 2071-7024

Stellmes M, Udelhoven T, Röder A, Sonnenschein R, Hill J, 2010. Dryland observation at local and regional scale - Comparison of Landsat TM/ETM+ and NOAA AVHRR time series. Remote Sensing of Environment 114(10): 211-225.

Sultan B, Roudier P, Traoré S, 2015. Les impacts du changement climatique sur les rendements agricoles en Afrique de l'Ouest. https://horizon.documentation.ird.fr › divers19-05

Tendeng M, Ndour N, Sambou B, Diatta M, Aouta A, 2016. Dynamique de la mangrove du marigot de Bignona autour du barrage d'Affiniam (Casamance, Sénégal). Int.J.Biol.Chem.Sci.10(2):666-680,2016.DOI: http://dx.doi.org/10.4314/ijbcs.v10i2.18

TraBi ZA, 2013. Étude de l'impact des activités anthropiques et de la variabilité climatique sur la végétation et les usages des sols, par utilisation de la télédétection et des statistiques agricoles, sur le bassin versant du Bouregreg (Maroc). Thèse de Doctorat, Université d'Artois (France), 189p.

Triki Fourati H, Bouaziz M, Benzina M, Bouaziz S, 2015. "Modeling of soil salinity within a semi-arid region using spectral analysis," Arabian J. Geosci., vol. 8, no. 12, pp. 11175–11182, 2015.

Zhang TT, Zeng SL, Gao Y, Ouyang ZT, Li B, Fang CM, Zhao B, 2011. Using hyperspectral vegetation indices as a proxy to monitor soil salinity. Ecol. Indic. 11 (6), 1552–1562.

Zhang Z, Fan Y, Zhang A. 2022 Baseline-Based Soil Salinity Index (BSSI): A Novel Remote Sensing Monitoring Method of Soil Salinization. IEEE J.

Sel. Topics Appl. Earth Observ. Remote Sens., vol. 16, 2023, pp. 203-214

Zoungrana BJ-B, Conrad C, Thiel M, Amekudzi LK, Dapola DE, 2018. MODIS NDVI trends and fractional land cover change for improved assessments of vegetation degradation in Burkina Faso, West Africa. Journal of Arid Environments, 153: 66 - 75.